

Adaptive Polarimetric Detection for MIMO Radar and Its Optimal Polarimetric Design in Compound-Gaussian Clutter

Zhikun Chen^{1, *} and Yinan Zhao²

Abstract—This study addresses the problem of adaptive polarimetric detector (APD) and optimal polarimetric design for the distributed multiple-input-multiple-output radar in compound-Gaussian clutter with inverse-gamma distributed texture component. We derive the APD by maximizing a posteriori estimation and performing a generalized likelihood ratio test. The false alarm probability for the detector is analyzed to validate the corresponding constant false alarm rate property. Furthermore, based on the concepts of game theory, we formulate an optimal polarimetric design as a two players zero-sum game, which further improves the performance of the proposed detector. Simulation results show that the proposed detector outperforms its counterparts, and the optimal polarimetric design algorithm can efficiently enhance the detection performance.

1. INTRODUCTION

Multiple-input-multiple-output (MIMO) radar with widely separated transmitting and receiving antennas is a new radar system that enables the viewing of the target from different angles. The echoes received by the antennas of a MIMO radar are approximately independent of each other (i.e., distributed MIMO radar) [1, 2]. Considering that the radar cross section (RCS) of a target is a function of the aspect angle, a distributed MIMO radar system can utilize spatial diversity to improve the detection performance. Several researchers have stated that MIMO radar is superior to other radar systems, such as phased array and single-input multiple-output radars in terms of detecting targets embedded in Gaussian clutter [3–11]. However, real-life clutter does not usually follow the Gaussian distribution for high-resolution radar in low-grazing angle [12, 13]. Therefore, several studies have developed detectors that are effective against K-distributed clutter [14–17].

To further improve the detection performance, researchers have introduced a new type of radar, which is the combination of polarimetric and distributed MIMO radars [18, 19]. To obtain the target polarimetric scattering information, polarimetric radar systems can transmit arbitrary polarization waveform matched with target's polarization [20]. The incorporation of the polarimetric diversity improves the performance of the MIMO radar [21–24]. One of the unique capabilities of the polarimetrically distributed MIMO radar is that each transmitter can choose its own polarimetric vector, and the properly designed vectors can improve the signal-to-noise ratio. For the APD, the polarization characteristics of the target can be changed according to the clutter. In this situation, the selection of polarization in such a MIMO radar remains a notable challenge. A polarimetric design method based on game theory is proposed in [25–27]. Unlike traditional adaptive polarimetric design methods, this kind of methods based on game theory does not need training data and can be easily implemented. However, the analysis on the optimal polarimetric design for distributed MIMO radar in compound-Gaussian (CG) clutter is seldom reported in relative publications.

Received 28 January 2020, Accepted 16 April 2020, Scheduled 11 May 2020

* Corresponding author: Zhikun Chen (czk@hdu.edu.cn).

¹ School of Automation, Hangzhou Dianzi University, Xiasha Higher Education Zone, 2nd Street, Hangzhou 310018, China. ² School of Electronics and Information Engineering, Harbin Institute of Technology, Harbin 150001, China.

In this study, we develop a generalized likelihood ratio test (GLRT) detector for polarimetric distributed MIMO radar in a CG clutter with inverse-gamma (i Γ) distributed texture component. First, we establish the signal model of the polarimetrically distributed MIMO radar. Second, an adaptive polarimetric detector (APD) is derived on the basis of this signal model. The combination of polarimetric and spatial diversity further improves the detection performance. Third, an optimal polarimetric design algorithm is incorporated to further improve the performance. Finally, several numerical examples are provided and evaluated to demonstrate the effectiveness of the proposed detector.

2. PROBLEM FORMULATION

2.1. Clutter Model

The CG family delivers an effective modeling of non-Gaussian clutter [28–30]. The general form of a CG vector can be expressed as

$$\mathbf{c} = \sqrt{\tau}\boldsymbol{\chi}, \quad (1)$$

where $\tau \in (0, \infty)$ is the texture component that has composite Gaussian distribution, and $\boldsymbol{\chi} \sim \mathcal{CN}(\mathbf{0}, \boldsymbol{\Sigma}) \in \mathbb{C}^N$ is the speckle. The texture is changing slowly, whereas the speckle is changing fast; these components are assumed to be independent.

For different members of the CG family, the texture components follow different distributions. This study adopts the i Γ distribution, and the corresponding model is named CG-i Γ . The PDF of the texture is defined as

$$f_{\tau}(\tau; \nu, \beta) = \frac{\beta^{\nu}}{\Gamma(\nu)} \tau^{-(\nu+1)} \exp\left(-\frac{\beta}{\tau}\right) 1_{(0, \infty)}(\tau). \quad (2)$$

where ν and β are the shape and rate parameters, respectively. Both are real positive numbers. To simplify the notation and derivation, we assume that the mean of the texture is equal to one (i.e., $\nu = \beta$), and the PDF can be simplified as follows:

$$f_{\tau}(\tau; \nu) = \frac{1}{\Gamma(\nu)} \nu^{\nu} \tau^{-(\nu+1)} \exp\left(-\frac{\nu}{\tau}\right) 1_{(0, \infty)}(\tau). \quad (3)$$

Given that the speckle is Gaussian-distributed with mean 0, see Equations (A7) and (A8) in Appendix A, the conditional PDF of the clutter vector can be expressed as

$$f_{\mathbf{c}|\tau}(\mathbf{c}|\tau) = \left(\det(\pi\tau\boldsymbol{\Sigma}) \exp\left(\|\mathbf{c}\|_{(\tau\boldsymbol{\Sigma})^{-1}}^2\right)\right)^{-1}. \quad (4)$$

Combining Equations (3) and (4) yields

$$f_{\mathbf{c}|\tau}(\mathbf{c}|\tau) f_{\tau}(\tau; \nu) = \frac{\nu^{\nu} \tau^{-\nu-1}}{\Gamma(\nu) \det(\pi\tau\boldsymbol{\Sigma})} \exp\left(-\frac{\|\mathbf{c}\|_{\boldsymbol{\Sigma}^{-1}}^2 + \nu}{\tau}\right) 1_{(0, \infty)}(\tau), \quad (5)$$

One of CG-i Γ 's advantages is that the closed form of the clutter's PDF can be obtained.

$$f_{\mathbf{c}}(\mathbf{c}; \nu) = \int_{-\infty}^{\infty} f_{\mathbf{c}|\tau}(\mathbf{c}|\tau) f_{\tau}(\tau; \nu) d\tau = \frac{\Gamma(\nu + N)}{\det(\pi\boldsymbol{\Sigma}) \nu^N \Gamma(\nu)} \left(1 + \frac{\|\mathbf{c}\|_{(\tau\boldsymbol{\Sigma})^{-1}}^2}{\nu}\right)^{-\nu-N}. \quad (6)$$

2.2. Signal Model

Assume that the target is a stationary point-like target with a scattering matrix that depends on the observing angle. The distributed MIMO radar comprises widely separated M transmitter and N receivers (Figure 1). Each transmitter and receiver have an antenna, which consists of a horizontally and a vertically polarized channel. The waveforms of the polarization channels are orthogonal to each other for any mutual delay to help the receivers separate the signals transmitted by the horizontally and vertically polarized antennas [31].

For each receiver, a bank consisting of M matched filters is used to separate the signals from different transmitters on the assumption that the waveforms transmitted by the M transmitters are

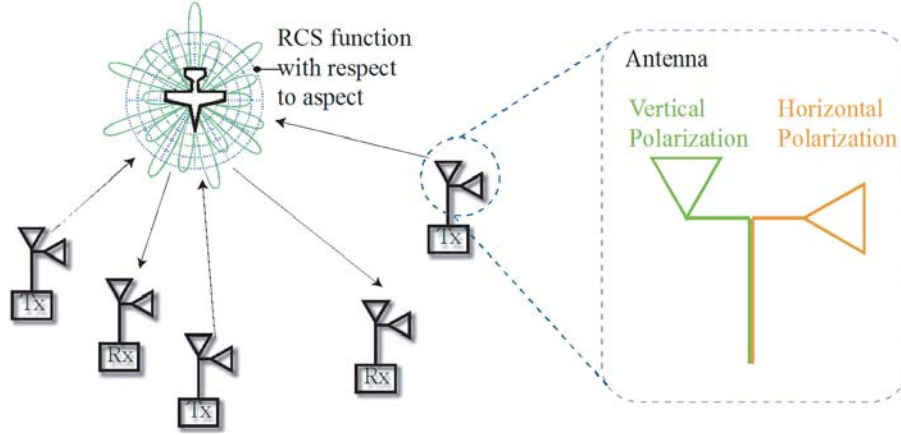


Figure 1. Distributed MIMO radar system.

orthogonal. Considering that each N receiver has two polarization channels, $2N$ matched filter banks are utilized in total, and the output of the filter banks corresponding to the l th range cell and k th pulse forms a vector on \mathbb{C}^{2MN} , which is represented as

$$\mathbf{y}_{k,l} = \mathbf{P}\mathbf{S}\mathbf{a}_{k,l} + \mathbf{c}_{k,l}, \quad (7)$$

where $\mathbf{c}_{k,l}$ is the clutter vector (the corresponding probability distribution function [PDF] is represented by Equation (3)), and the speckle components of $\mathbf{c}_{k,l}$, $k = 1, 2, \dots, K$ are mutually independent [30]. \mathbf{P} is the polarimetric matrix, which is defined as

$$\mathbf{P} = \text{Diag} \left(\mathbf{I}_N \otimes \tilde{\mathbf{P}}_m \right), \quad m = 1, 2, \dots, M, \quad (8)$$

where $\tilde{\mathbf{P}}_m$ can be expressed as

$$\tilde{\mathbf{P}}_m = \text{Diag} (\mathbf{p}_m) \begin{pmatrix} 1 & 1 & 0 & 0 \\ 0 & 0 & 1 & 1 \end{pmatrix}; \quad (9)$$

\mathbf{p}_m denotes the polarimetric vector of the m th transmitter, which satisfies $\|\mathbf{p}_m\| = 1$ for each $m \in \{1, 2, \dots, M\}$. Matrix \mathbf{S} represents the polarimetric property of the target, which is defined as

$$\mathbf{S} = \text{Diag} \left(\text{vec} \left(\tilde{\mathbf{S}}_{1,1} \right), \dots, \text{vec} \left(\tilde{\mathbf{S}}_{1,N} \right), \dots, \text{vec} \left(\tilde{\mathbf{S}}_{M,1} \right), \dots, \text{vec} \left(\tilde{\mathbf{S}}_{M,N} \right) \right), \quad (10)$$

where $\tilde{\mathbf{S}}_{m,n} \in \mathbb{C}^{2 \times 2}$ is the polarimetric scattering matrix (PSM) of the target corresponding to the m th transmitter and n th receiver, and \mathbf{a}_k is the complex magnitude of the target echo.

$$\mathbf{a}_k = (a_{1,1}, \dots, a_{1,N}, \dots, a_{M,1}, \dots, a_{M,N})^T. \quad (11)$$

where $a_{M,N}$ denotes the complex magnitude of the signal transmitted by the m th transmitter, reflected by the target, and received by the n th receiver. To simplify the notation, we specify that the index of the cell under test (CUT) is $l = 1$ (i.e., $\mathbf{y}_{k,1}$ is the primary data from the CUT). We also adopt the data from the L range cells, which are spatially adjacent to the CUT and denoted by $\{\mathbf{y}_{k,l} : l = 2 \dots L + 1\}$, in which no target is present. Moreover, the spectral properties of the clutter are the same to that of CUT.

3. APD FOR MIMO RADAR AND OPTIMAL POLARIMETRIC DESIGN IN COMPOUND-GAUSSIAN CLUTTER

Based on the signal model provided in the previous section, the detection of a point target embedded in the CG-i Γ clutter can be modeled as a binary hypothesis test. The hypothesis is defined below.

$$H_\lambda : \mathbf{y}_{k,l} = \lambda \delta_{l-1} \mathbf{P}\mathbf{S}\mathbf{a}_{k,l} + \mathbf{c}_{k,l}. \quad (12)$$

where $l \in \{1, 2, \dots, L+1\}$, $k \in \{1, 2, \dots, K\}$, $\lambda \in \{0, 1\}$, and H_λ denotes the null hypothesis if $\lambda = 0$ or the alternative hypothesis if $\lambda = 1$. From Equation (A8) in Appendix A, the conditional PDF of $\mathbf{y}_{k,1}$ is expressed as

$$f(\mathbf{y}_{k,1} | \mathbf{a}_k, \tau_k; H_\lambda) = \left(\det(\pi \tau_k \boldsymbol{\Sigma}) \left(\exp \circ \text{dist}_{M(\tau_k \boldsymbol{\Sigma})}^2 \right) (\mathbf{y}_{k,1}, \lambda \mathbf{P} \mathbf{S} \mathbf{a}_k) \right)^{-1}. \quad (13)$$

where τ_k is the texture component corresponding to the k th pulse. The corresponding PDF is shown in Equation (3).

3.1. GLRT Derivation

In this section, we utilize the two-step GLRT method to derive the APD, and the unknown parameters are replaced with the estimated values.

Step 1: Assume that the texture component is known, and the detector can be expressed as follows:

$$\prod_{k=1}^K \frac{f(\mathbf{y}_{k,1} | \hat{\mathbf{a}}_k, \tau_k; H_1)}{f(\mathbf{y}_{k,1} | \tau_k; H_0)} \underset{H_0}{\overset{H_1}{\geq}} \ln \gamma. \quad (14)$$

where $\hat{\mathbf{a}}_k$ is the maximum likelihood estimation (MLE) of \mathbf{a}_k . Considering that the signal model in [32] is linear, the MLE is equivalent to the generalized least squares, which can be expressed by the projection problem in Appendix A

$$\mathbf{P} \mathbf{S} \hat{\mathbf{a}}_k = \text{proj}_{M(\boldsymbol{\Sigma})}(\mathbf{y}_{k,1}, \text{col}(\mathbf{P} \mathbf{S})). \quad (15)$$

By substituting Equation (A13) in Appendix A, into Equation (15), the estimator is defined as

$$\hat{\mathbf{a}}_k = \left((\mathbf{P} \mathbf{S})^H \boldsymbol{\Sigma}^{-1} \mathbf{P} \mathbf{S} \right)^{-1} (\mathbf{P} \mathbf{S})^H \boldsymbol{\Sigma}^{-1} \mathbf{y}_{k,1}. \quad (16)$$

By substituting Equations (13) and (15) into Equation (14), the detector can be equivalently written as

$$\sum_{k=1}^K \frac{1}{\tau_k} \left(\|\mathbf{y}_{k,1}\|_{\boldsymbol{\Sigma}^{-1}}^2 - \text{dist}_{M(\boldsymbol{\Sigma})}^2(\mathbf{y}_{k,1}, \text{proj}_{M(\boldsymbol{\Sigma})}(\mathbf{y}_{k,1}, \text{col}(\mathbf{P} \mathbf{S})) \right) \right) \underset{H_0}{\overset{H_1}{\geq}} \ln \gamma. \quad (17)$$

On the basis of Theorem II in Appendix A, the expression can be further simplified as

$$\sum_{k=1}^K \frac{\left\| \text{proj}_{M(\boldsymbol{\Sigma})}(\mathbf{y}_{k,1}, \text{col}(\mathbf{P} \mathbf{S})) \right\|_{\boldsymbol{\Sigma}^{-1}}^2}{\tau_k} \underset{H_0}{\overset{H_1}{\geq}} \ln \gamma. \quad (18)$$

Step 2: Determine the maximum posteriori estimator of τ_k by solving the following equation:

$$\{\hat{\tau}_k : k = 1 \dots K\} = \max_{\{\hat{\tau}_k : k=1 \dots K\}} \prod_{k=1}^K f(\mathbf{y}_{k,1} | \mathbf{a}_k, \tau_k; H_\lambda) f_{\tau_k}(\hat{\tau}_k). \quad (19)$$

By assuming that $\tau_k, k = 1 \dots K$ are mutually independent, the estimator can be obtained by solving the following equation:

$$\frac{\partial f(\mathbf{y}_{k,1} | \mathbf{a}_k, \tau_k; H_\lambda) f_{\tau_k}(\tau_k; \nu)}{\partial \tau_k} = 0, \quad k = 1 \dots K. \quad (20)$$

Substituting Equations (3), (A8), and (13) into the left-hand side (LHS) of Equation (20) yields

$$\begin{aligned} & \frac{\partial f(\mathbf{y}_{k,1} | \mathbf{a}_k, \tau_k; H_\lambda) f_{\tau_k}(\tau_k; \nu)}{\partial \tau_k} \\ &= \frac{\partial}{\partial \tau_k} \Gamma^{-1}(\nu) \nu^\nu \det^{-1}(\pi \boldsymbol{\Sigma}) \tau_k^{-2MN - \nu - 1} \exp \left(- \frac{\text{dist}_{M(\boldsymbol{\Sigma})}^2(\mathbf{y}_{k,1}, \lambda \mathbf{P} \mathbf{S} \mathbf{a}_k) + \nu}{\tau_k} \right) \\ &= \Gamma^{-1}(\nu) \nu^\nu \det^{-1}(\pi \boldsymbol{\Sigma}) \exp \left(- \frac{\text{dist}_{M(\boldsymbol{\Sigma})}^2(\mathbf{y}_{k,1}, \lambda \mathbf{P} \mathbf{S} \mathbf{a}_k) + \nu}{\tau_k} \right) \\ & \times \left(\frac{\text{dist}_{M(\boldsymbol{\Sigma})}^2(\mathbf{y}_{k,1}, \lambda \mathbf{P} \mathbf{S} \mathbf{a}_k) + \nu - (2MN + \nu + 1) \tau_k}{\tau_k^{2MN + \nu + 3}} \right). \end{aligned} \quad (21)$$

Substituting Equation (21) into Equation (20), the solution of the equation is as follows:

$$\hat{\tau}_{k;H_\lambda} = \frac{\text{dist}_{M(\Sigma)}^2(\mathbf{y}(k), \lambda \mathbf{PSa}_k) + \nu}{2MN + \nu + 1}. \quad (22)$$

Unknown covariance matrix Σ can be estimated using secondary data [32].

$$\hat{\Sigma} = \frac{1}{KL} \sum_{l=2}^{L+1} \sum_{k=1}^K \frac{\mathbf{y}_{k,l} \mathbf{y}_{k,l}^H}{\|\mathbf{y}_{k,l}\|^2}. \quad (23)$$

Substituting $\hat{\tau}_{k;H_0}$ and $\hat{\Sigma}$ into Equation (18), we obtain

$$\sum_{k=1}^K \frac{\left\| \text{proj}_{M(\hat{\Sigma})}(\mathbf{y}_{k,1}, \text{col}(\mathbf{PS})) \right\|_{\hat{\Sigma}^{-1}}^2}{\|\mathbf{y}_{k,1}\|_{\hat{\Sigma}^{-1}}^2 + \nu} \underset{H_0}{\overset{H_1}{\geq}} \gamma'. \quad (24)$$

where $\gamma' = \ln \gamma / 2MN + \nu + 1$. According to Theorem I in Appendix A, the numerator of the LHS of Equation (24) can be simplified as follows:

$$\left\| \text{proj}_{M(\hat{\Sigma})}(\mathbf{y}_{k,1}, \text{col}(\mathbf{PS})) \right\|_{\hat{\Sigma}^{-1}}^2 = \left\langle \mathbf{y}_{k,1}, \text{proj}_{M(\hat{\Sigma})}(\mathbf{y}_{k,1}, \text{col}(\mathbf{PS})) \right\rangle_{\hat{\Sigma}^{-1}} = \mathbf{y}_{k,1}^H \Phi \mathbf{y}_{k,1}, \quad (25)$$

where

$$\Phi = \hat{\Sigma}^{-1} \text{proj}_{M(\hat{\Sigma})}(\mathbf{y}_{k,1}, \text{col}(\mathbf{PS})) = \Sigma^{-1} \mathbf{PS} \left((\mathbf{PS})^H \Sigma^{-1} \mathbf{PS} \right)^{-1} (\mathbf{PS})^H \Sigma^{-1}. \quad (26)$$

3.2. Constant False Alarm Rate (CFAR) Analysis

The PDF of the test statistic should be derived to analyze the CFAR property of the proposed detector. Assuming that the covariance matrix of the speckle is a known priori information, according to Theorem IV in Appendix A, we can obtain

$$\left\| \text{proj}_{M(\Sigma)}(\mathbf{y}_{k,1}, \text{col}(\mathbf{PS})) \right\|_{\Sigma^{-1}}^2 \sim \chi^2(2\text{rank}(\mathbf{PS})). \quad (27)$$

However, the covariance matrix is unknown in the scenario in this study, and the estimated value from Equation (23) is used, which is complicated for the problem. For simplicity, we denote the test statistic in Equation (24) as Δ , where

$$\Delta = \sum_{k=1}^K \frac{\left\| \text{proj}_{M(\hat{\Sigma})}(\mathbf{y}_{k,1}, \text{col}(\mathbf{PS})) \right\|_{\hat{\Sigma}^{-1}}^2}{\|\mathbf{y}_{k,1}\|_{\hat{\Sigma}^{-1}}^2 + \nu}. \quad (28)$$

According to Equation (A8) in Appendix A, if $K = 1$ and $\nu = 1$, then Δ can be equivalently written as

$$\Delta = g(\zeta), \quad g(\zeta) = (1 + \zeta)^{-1}, \quad (29)$$

where random variable ζ follows the F distribution, that is, $\zeta \sim \mathcal{F}(2(L - 2MN + 1), 4MN)$. The corresponding PDF is defined as

$$f_\zeta(\zeta) = \frac{\Gamma\left(\frac{n_1 + n_2}{2}\right)}{\Gamma\left(\frac{n_1}{2}\right) \Gamma\left(\frac{n_2}{2}\right)} (n_1)^{n_1/2} (n_2)^{n_2/2} \frac{\zeta^{n_1/2-1}}{(n_1\zeta + n_2)^{\frac{n_1+n_2}{2}}} 1_{[0,\infty)}(\zeta), \quad (30)$$

where $n_1 = 2(L - 2MN + 1)$ and $n_2 = 4MN$. Considering that the Δ from Equation (29) is a function with respect to ζ , the PDF is then expressed as

$$f_\Delta(\Delta) = f_\zeta(g^{-1}(\Delta)) \left| \frac{dg^{-1}(\Delta)}{d\Delta} \right| = f_\zeta\left(\frac{1-\Delta}{\Delta}\right) \Delta^{-2}. \quad (31)$$

According to [28], the PDF of the test statistic for an arbitrary K is represented by the following expression on the assumption that $\mathbf{y}_{k,1}$, $k = 1 \dots K$ is mutually independent.

$$f_{\Delta}(\Delta) = f_{\zeta}\left(\frac{1-\Delta}{\Delta}\right) \Delta^{-2} * f_{\zeta}\left(\frac{1-\Delta}{\Delta}\right) \Delta^{-2} * \dots * f_{\zeta}\left(\frac{1-\Delta}{\Delta}\right) \Delta^{-2}. \quad (32)$$

Thus, the false alarm probability can be calculated as follows:

$$\mathcal{P}_{FA} = \Pr(\Delta > \gamma' | H_1) = \int_{\gamma}^{\infty} f_{\Delta}(\Delta) d\Delta = \int_0^{\frac{1-\gamma'}{\gamma'}} f_{\zeta}(\zeta) d\zeta, \quad (33)$$

which is independent of the clutter power and the structure of the clutter's covariance matrix, that is, the proposed detector has a CFAR. However, random variable ζ is not guaranteed to follow the F distribution for arbitrary ν , indicating that the \mathcal{P}_{FA} of the proposed detector depends on the shape parameter of the clutter. Thus, the detector does not have a CFAR with respect to ν , which is consistent with a previous report [33]. Fortunately, ν is usually constant in a given scenario with a fixed grazing angle and sea state.

3.3. Optimal Polarimetric Design

Considering that the transmitters and receivers have horizontal and vertical polarization channels, promoting the system performance by transmitting a polarized waveform, where the polarimetric vector matches the PSM of the target, is possible. However, the PSM of the target in the current scene is an unknown priori information in many practical applications. Therefore, many traditional polarimetric design methods estimate the PSM of the target by utilizing training data. The authors of [20] suggested that the polarimetric design problem for detecting targets embedded in Gaussian clutter can be solved using a game theory-based algorithm without using training data. In this study, we demonstrate that game theory can also be used in iF-CG clutter scenarios.

In the context of game theory, two players are present for the optimal polarimetric design problem. Player 2 is the radar engineer who intends to maximize the radar performance, whereas player 1 is the opponent who degrades the radar performance. This game is classified as a two-person zero-sum game, in which the sum of the players' payoff function is zero for a given strategy pair. As defined by the Game Theory, the two zero sum has the following rules:

Rule 1: The number of players is assumed as a prior information;

Rule 2: As a result of the game, the total profit of the single objective is not required to be a constant (non-zero-sum).

In our approach, there are two players. They separately have their own profit (objective) to be maximized under their cooperation. The process can be described in detail as follows:

Given that M transmitters can independently choose the polarimetric vector, the optimal polarimetric design comprises M independent games. For the m th transmitter, the strategy set of player 2 is a group of polarimetric vectors for each transmitter.

$$S_2 = \{\mathbf{p}_m(x_2) : x_2 = 1, 2, \dots, X_2\}. \quad (34)$$

where X_2 is the total number of vectors. For player 1, we assume that the PSM of the target is random and follows the Gaussian distribution with covariance matrix $\mathbf{\Xi}$, that is, $\text{vec}(\tilde{\mathbf{S}}_{m,n}) \sim \mathcal{CN}(\mathbf{0}, \mathbf{\Xi})$. If the X_1 types of targets with different polarization characteristics exist, then the strategy set of player 1 is a group of covariance matrices.

$$S_1 = \{\mathbf{\Xi}_{m,n}(x_1) : m = 1, 2, \dots, M, n = 1, 2, \dots, N, x_1 = 1, 2, \dots, X_1\}, \quad (35)$$

where $\mathbf{\Xi}_{m,n}(x_1)$ denotes the covariance matrix of $\text{vec}(\tilde{\mathbf{S}}_{m,n})$ of target type a . The payoff function of player 2 corresponding to the m th transmitter is defined by the power of the signal component.

$$u_2(\mathbf{\Xi}_m(x_1), \mathbf{p}_m(x_2)) = E \left\{ \left\| \mathbf{I}_N \otimes \text{Diag}(\mathbf{p}_m(x_2)) \begin{pmatrix} 1 & 1 & 0 & 0 \\ 0 & 0 & 1 & 1 \end{pmatrix} \times \text{Diag}(\text{vec}(\tilde{\mathbf{S}}_{m,1}), \dots, \text{vec}(\tilde{\mathbf{S}}_{m,N})) \begin{bmatrix} \alpha_{m,1} & \alpha_{m,2} & \dots & \alpha_{m,N} \end{bmatrix}^T \right\|^2 \right\}. \quad (36)$$

The game is a zero-sum game. Hence, the payoff function of player 1 corresponding to the m th transmitter is expressed as

$$u_1(\mathbf{E}_m(x_1), \mathbf{p}_m(x_2)) = -u_2(\mathbf{E}_m(x_1), \mathbf{p}_m(x_2)). \quad (37)$$

When the critical components of a game, including the players, strategies, and payoff functions, have been defined, the optimal polarimetric design problem can be solved by the method as in [23].

4. SIMULATION ANALYSIS

Several numerical examples are provided in this section to evaluate the performance of the proposed detector. The software platform for the simulation is MATLAB, and the operations are performed using double precision floating point numbers. The number of the pulses during an observation time is $K = 40$; and the number of the training data is $L = 20$. The false alarm probability of the detector is set to $\mathcal{P}_{FA} = 10^{-3}$, and the number of independent repeated trails is $100/\mathcal{P}_{FA}$. The target-to-clutter ratio (TCR) is defined as

$$\text{TCR} = \frac{1}{2K} \frac{\sum_{k=1}^K \|\mathbf{P}\mathbf{S}\mathbf{a}_k\|^2}{E\{\tau_k\} \text{tr}(\mathbf{\Psi})}, \quad (38)$$

where $\mathbf{\Psi}$ is the spatial covariance matrix of the speckle components, which are defined as follows:

$$\mathbf{\Psi} = \text{Diag}(\mathbf{\Psi}_1, \mathbf{\Psi}_2, \dots, \mathbf{\Psi}_M), \quad (39)$$

$$(\mathbf{\Psi}_m)_{p,q} = \rho_s^{|p-q|}, \quad m = 1, 2, \dots, M, \quad p, q = 1, 2, \dots, N, \quad (40)$$

where $\rho_s = 0.01$ is the spatial correlation coefficient.

4.1. Performance Analysis

In this example, two transmitters and four receivers are involved. The covariance matrices of the target's PSM are expressed as

$$\begin{aligned} \mathbf{E}_{1,1} &= \begin{pmatrix} 0.6 & 0.1\varepsilon & 0.1\varepsilon & 0.1\varepsilon \\ 0.1\varepsilon^* & 0.3 & 0.1\varepsilon & 0.1\varepsilon \\ 0.1\varepsilon^* & 0.1\varepsilon^* & 0.2 & 0.1\varepsilon \\ 0.1\varepsilon^* & 0.1\varepsilon^* & 0.1\varepsilon^* & 0.4 \end{pmatrix}, & \mathbf{E}_{1,2} &= \begin{pmatrix} 0.4 & 0.05\varepsilon & 0.05\varepsilon & 0.05\varepsilon \\ 0.05\varepsilon^* & 0.2 & 0.05\varepsilon & 0.05\varepsilon \\ 0.05\varepsilon^* & 0.05\varepsilon^* & 0.5 & 0.05\varepsilon \\ 0.05\varepsilon^* & 0.05\varepsilon^* & 0.05\varepsilon^* & 0.4 \end{pmatrix}, \\ \mathbf{E}_{1,3} &= \begin{pmatrix} 0.3 & 0.1\varepsilon & 0.1\varepsilon & 0.1\varepsilon \\ 0.1\varepsilon^* & 0.4 & 0.1\varepsilon & 0.1\varepsilon \\ 0.1\varepsilon^* & 0.1\varepsilon^* & 0.3 & 0.1\varepsilon \\ 0.1\varepsilon^* & 0.1\varepsilon^* & 0.1\varepsilon^* & 0.5 \end{pmatrix}, & \mathbf{E}_{1,4} &= \begin{pmatrix} 0.3 & 0.05\varepsilon & 0.05\varepsilon & 0.05\varepsilon \\ 0.05\varepsilon^* & 0.5 & 0.05\varepsilon & 0.05\varepsilon \\ 0.05\varepsilon^* & 0.05\varepsilon^* & 0.4 & 0.05\varepsilon \\ 0.05\varepsilon^* & 0.05\varepsilon^* & 0.05\varepsilon^* & 0.2 \end{pmatrix}, \\ \mathbf{E}_{2,1} &= \begin{pmatrix} 0.2 & 0.1\varepsilon & 0.1\varepsilon & 0.1\varepsilon \\ 0.1\varepsilon^* & 0.4 & 0.1\varepsilon & 0.1\varepsilon \\ 0.1\varepsilon^* & 0.1\varepsilon^* & 0.3 & 0.1\varepsilon \\ 0.1\varepsilon^* & 0.1\varepsilon^* & 0.1\varepsilon^* & 0.4 \end{pmatrix}, & \mathbf{E}_{2,2} &= \begin{pmatrix} 0.6 & 0.05\varepsilon & 0.05\varepsilon & 0.05\varepsilon \\ 0.05\varepsilon^* & 0.3 & 0.1\varepsilon & 0.05\varepsilon \\ 0.05\varepsilon^* & 0.05\varepsilon^* & 0.4 & 0.05\varepsilon \\ 0.05\varepsilon^* & 0.05\varepsilon^* & 0.05\varepsilon^* & 0.4 \end{pmatrix}, \\ \mathbf{E}_{2,3} &= \begin{pmatrix} 0.5 & 0.1\varepsilon & 0.1\varepsilon & 0.1\varepsilon \\ 0.1\varepsilon^* & 0.3 & 0.1\varepsilon & 0.1\varepsilon \\ 0.1\varepsilon^* & 0.1\varepsilon^* & 0.3 & 0.1\varepsilon \\ 0.1\varepsilon^* & 0.1\varepsilon^* & 0.1\varepsilon^* & 0.4 \end{pmatrix}, & \mathbf{E}_{2,4} &= \begin{pmatrix} 0.3 & 0.05\varepsilon & 0.05\varepsilon & 0.05\varepsilon \\ 0.05\varepsilon^* & 0.4 & 0.05\varepsilon & 0.05\varepsilon \\ 0.05\varepsilon^* & 0.05\varepsilon^* & 0.5 & 0.05\varepsilon \\ 0.05\varepsilon^* & 0.05\varepsilon^* & 0.05\varepsilon^* & 0.3 \end{pmatrix}. \end{aligned}$$

where $\varepsilon = 1 + \sqrt{-1}$. The polarimetric vector of the transmitters is expressed as

$$\mathbf{p}_m = [1 \ 0]^T, \quad m = 1, 2. \quad (41)$$

First, we compare the detection performance of the proposed APD and a non-adaptive polarimetric detector (NAPD) with prior knowledge on the clutter. The detection probability with respect to TCR (Equation (38)) is illustrated in Figure 2, which shows that the APD can obtain high detection

performance even in a strong clutter environment. APD is inferior to NAPD due to the lack of clutter knowledge. However, clutter knowledge is usually unknown in practical scenarios, which means that the former is more suitable for practical use than the latter. Second, we compare the performance of the APD with the corresponding single-polarized version. The number of the receivers is $N = 2, 3, 4$, and the shape parameter is $\nu = 1$. The detection probability with respect to TCR is displayed in Figure 3. The performance improves as the number of receiver increases. The detection performance increases by approximately 3 dB when many receivers are used, and the horizontal and vertical polarization channels are utilized. Finally, we analyze the CFAR property of the APD against fluctuating clutter. The PDF of texture component τ is defined in Equation (2), and the false alarm probability with respect to $E\{\tau\}$ is illustrated in Figure 4. The obtained curves imply that the APD has a CFAR for a fixed-shape

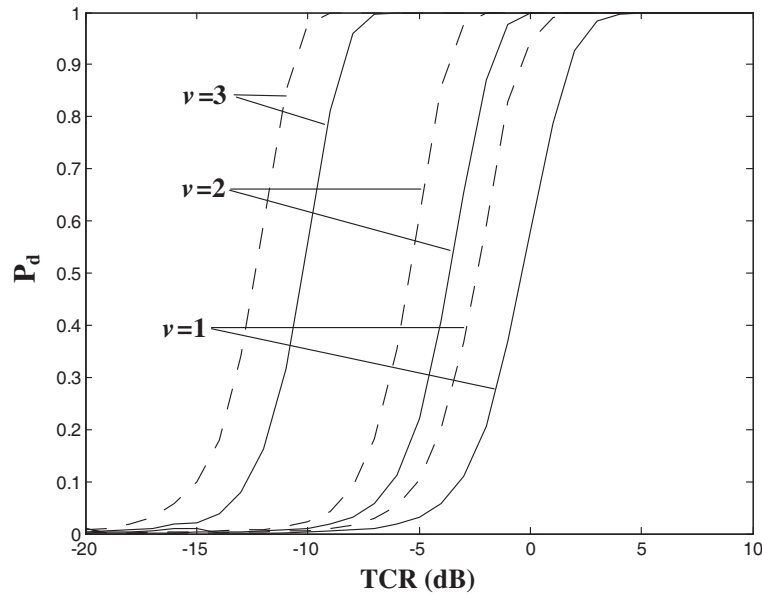


Figure 2. Detection probability of the APD (solid line) and NAPD (dashed line).

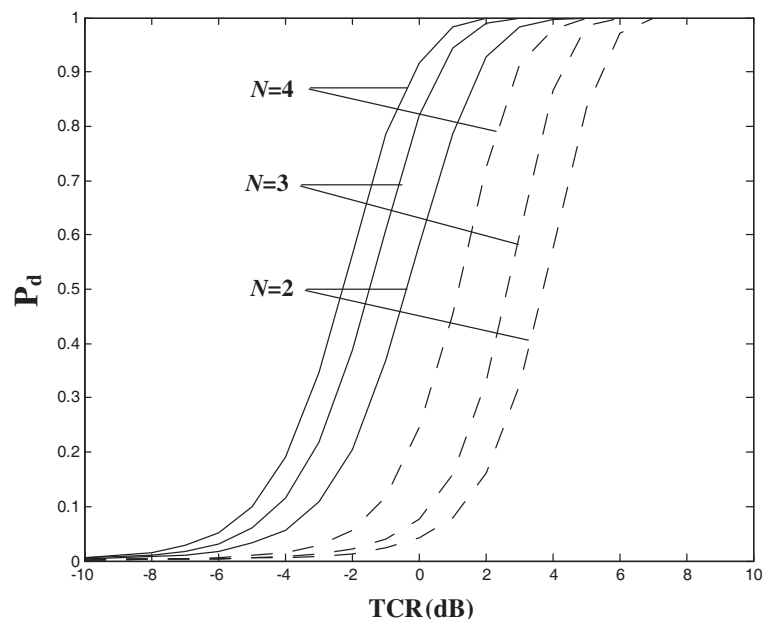


Figure 3. Detection probability of the dual-(solid line) and single-polarized (dashed line) APDs.

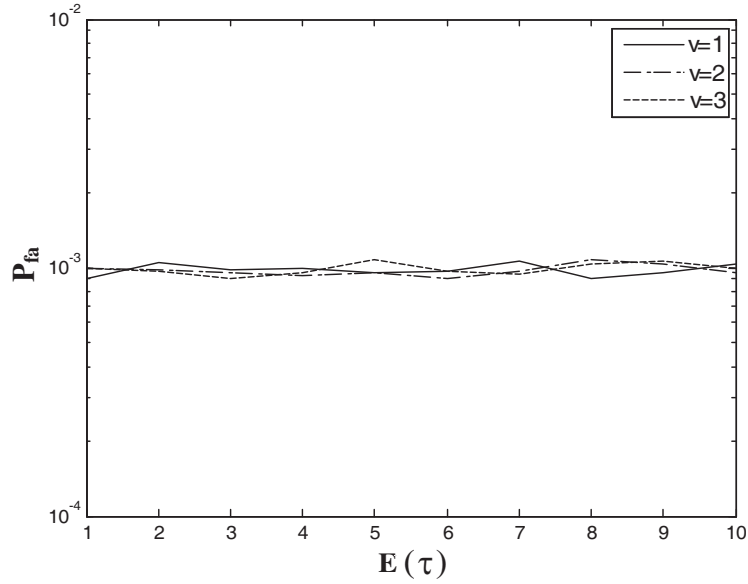


Figure 4. False alarm probability versus the mean of texture component.

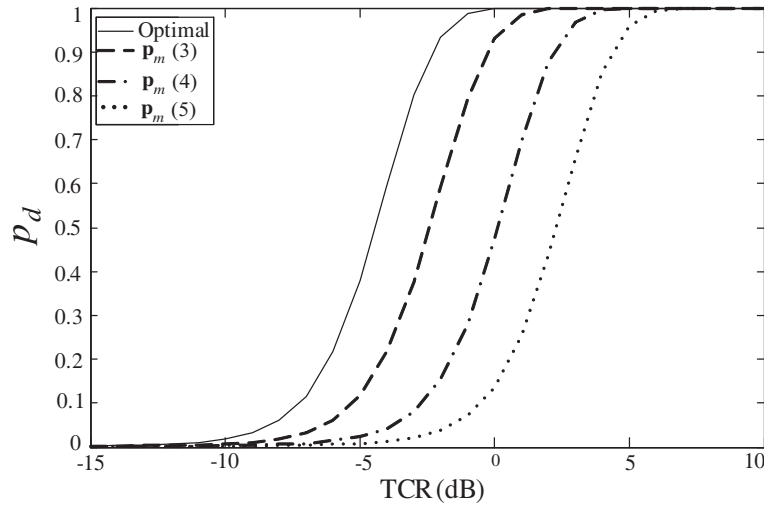


Figure 5. Detection probability of the APD using different polarimetric vectors.

parameter, which is consistent with the derivation in Subsection 3.2.

4.2. Example of an Optimal Polarimetric Design based on Game Theory

The numbers of the transmitters and receivers are $M = N = 2$, and five candidates for the optimal polarimetric vector are considered.

$$\begin{aligned}
 \mathbf{p}_m(1) &= (1 \ 0)^T \\
 \mathbf{p}_m(2) &= (0 \ 1)^T \\
 \mathbf{p}_m(3) &= (0.4082 + j0.5774, 0.4082 + j0.5774)^T \\
 \mathbf{p}_m(4) &= (0.4954 + j0.6396, 0.3055 + j0.5022)^T \\
 \mathbf{p}_m(5) &= (0.3166 + j0.5351, 0.4522 + j0.6395)^T.
 \end{aligned} \tag{42}$$

For player 1, two possible types of target are available, and the corresponding covariance matrix is provided in [23]. The probabilities of the two types of target are 0.3046 and 0.6954. By utilizing

the technique on the basis of game theory, the optimal polarimetric vector can be determined as the mixture of $\mathbf{p}_m(1)$ and $\mathbf{p}_m(2)$. The detection probability is displayed in Figure 5. The result shows that the designed polarimetric vector is superior to the candidates in the detecting targets.

5. CONCLUSIONS

Unlike conventional radars, a polarimetric distributed MIMO radar can utilize spatial and polarimetric diversity. In this study, we attempt to realize the full potential of polarimetric diversity by deriving the APD combined with a game theory-based optimal polarimetric design method. The derivation of the detector is based on a Mahalanobis projector, which whitens the clutter, and a CG model, which allows the proposed detector to deal with non-Gaussian clutter. In scenarios where the PSM of the target is unknown, the method based on game theory can help the radar identify the most suitable polarimetric vector from several candidate vectors. The numerical examples have demonstrated the usage of the detector, and the result reveals that the detection performance is satisfactory on the specified radar scene.

6. DECLARATIONS

The authors declare that there is no conflict of interests regarding the publication of this article.

ACKNOWLEDGMENT

The authors would like to thank Dr. Fengcong Li for proofreading the manuscript and valuable suggestions about the recovered procedure in the paper. This work was supported by the National Natural Science Foundation of China, Grant number [No. 61701148; No. 6170313; No. 61703128 and 61703129].

APPENDIX A.

Important mathematical operator' notation and theorems

Assuming that j denotes the imaginary unit of vectors, we let $\varepsilon = 1 + j$. The gamma function is denoted by $\Gamma(\cdot)$, and $E\{\cdot\}$ denotes the statistical expectation operation. For a set S , $\text{card}(S)$ denotes its cardinality, and 1_S denotes its indicator function, defined as follows:

$$1_S(x) = \begin{cases} 1 & x \in S \\ 0 & x \notin S \end{cases} \quad (\text{A1})$$

By utilizing the indicator function, we define the Kronecker delta as follows:

$$\delta_n = 1_{\{0\}}(n), \quad n \in \mathbb{Z}. \quad (\text{A2})$$

For functions/operators f and g , $f \circ g$ denotes the composition, shown as follows:

$$(f \circ g)(x) = f(g(x)). \quad (\text{A3})$$

The **iterative function** is denoted by $(f)^K$, defined as follows:

$$(f)^K(x) = \begin{cases} ((f)^{K-1} \circ f)(x) & K > 0 \\ x & K = 0 \end{cases}. \quad (\text{A4})$$

We denote vector and matrices with boldface lower and upper case letters, respectively. The operator \otimes denotes the Kronecker product. The transpose operator is denoted by $(\cdot)^T$, while the element-wise conjugate and Hermitian transpose operation are denoted by $(\cdot)^*$ and $(\cdot)^H$, respectively. The operator $\text{tr}\{\cdot\}$ represents the trace of a given square matrix, and $\text{rank}(\cdot)$ denotes the given matrix's rank. The operator $\text{Diag}(\cdot)$ is used to construct diagonal or block diagonal matrices; if the parameter of $\text{Diag}(\cdot)$ is a vector, $\text{Diag}(\cdot)$ forms a diagonal matrix from the elements of the vector; $\text{Diag}(\cdot)$ forms

a block diagonal matrix if its parameters are several vectors or matrices. The operator $\text{vec}(\cdot)$ denotes a vector formed by stacking the column vectors of the given matrix. \mathbf{I}_N is an $N \times N$ identity matrix. The element of matrix \mathbf{X} located at the n th row and m th column is denoted by $(\mathbf{X})_{m,n}$.

The Euclidian norm of a vector is denoted by $\|\cdot\|$, while $\|\cdot\|_{\mathbf{C}}$ denotes the weighted norm, defined as follows:

$$\|y\|_{\mathbf{C}} = \sqrt{\langle y, y \rangle_{\mathbf{C}}}, \tag{A5}$$

where \mathbf{C} is a positive definite Hermitian matrix, i.e., $\mathbf{C} \succ 0$, and $\langle \cdot, \cdot \rangle_{\mathbf{C}}$ denotes the weighted inner product, defined as follows:

$$\langle \mathbf{x}, \mathbf{y} \rangle_{\mathbf{C}} = \mathbf{x}^H \mathbf{C} \mathbf{y} \tag{A6}$$

Based on the weighted norm, we introduce the Mahalanobis distance which is a powerful tool for describing Gaussian and compound-Gaussian problems:

$$\text{dist}_{M(\mathbf{C})}(\mathbf{x}, \mathbf{y}) = \|\mathbf{x} - \mathbf{y}\|_{\mathbf{C}^{-1}} = \sqrt{(\mathbf{x} - \mathbf{y})^H \mathbf{C}^{-1} (\mathbf{x} - \mathbf{y})}. \tag{A7}$$

By utilizing the Mahalanobis distance [27], the probability density function (PDF) of the complex circular Gaussian distribution $\mathcal{CN}(\mu, \mathbf{C})$ can be expressed as:

$$f(\mathbf{x}) = \left(\det(\pi \mathbf{C}) \left(\exp \circ \text{dist}_{M(\mathbf{C})}^2(\mathbf{x}, \mu) \right) \right)^{-1}, \tag{A8}$$

where $\det(\cdot)$ denotes the determinant of a given square matrix.

For a space in which the distance $\text{dist}(\cdot, \cdot)$ is defined, we can introduce the concept of **projection**, defined as follows:

$$\text{proj}(\mathbf{b}, \text{col}(\mathbf{G})) = \arg \min_{\mathbf{g} \in \text{col}(\mathbf{G})} \text{dist}(\mathbf{b}, \mathbf{g}). \tag{A9}$$

where \mathbf{G} is a complex matrix; $\text{col}(\mathbf{G})$ denotes the column space of \mathbf{G} , and \mathbf{g} is a complex vector on $\text{col}(\mathbf{G})$, which means that \mathbf{g} is the linear combination of the column vectors of \mathbf{G} , i.e.,

$$\mathbf{g} = \mathbf{G} \alpha, \tag{A10}$$

where α is a complex vector. The definition shown in Equation (9) is abstract since the distance is not defined explicitly. By substituting Euclidean distance into Eq. (9), we have the projector on Euclidean space, shown as follows:

$$\text{proj}_E(\mathbf{b}, \text{col}(\mathbf{G})) = \arg \min_{\mathbf{g} \in \text{col}(\mathbf{G})} \|\mathbf{b} - \mathbf{g}\| = \mathbf{G} (\mathbf{G}^H \mathbf{G})^{-1} \mathbf{G}^H \mathbf{b}. \tag{A11}$$

Another expression of the projector can be obtained by substituting the Mahalanobis distance into Eq. (9), shown as follows:

$$\text{proj}_{M(\mathbf{C})}(\mathbf{b}, \text{col}(\mathbf{G})) = \arg \min_{\mathbf{g} \in \text{col}(\mathbf{G})} \text{dist}_{M(\mathbf{C})}(\mathbf{b}, \mathbf{g}). \tag{A12}$$

To solve the equation shown in Eq. (A12), substituting Eq. (A10) into Eq. (A12), we have the following generalized least squares (GLS) problem:

$$\min_{\alpha} (\mathbf{b} - \mathbf{G} \alpha)^H \mathbf{C}^{-1} (\mathbf{b} - \mathbf{G} \alpha), \tag{A13}$$

and the solution is $\alpha = (\mathbf{G}^H \mathbf{C}^{-1} \mathbf{G})^{-1} \mathbf{G}^H \mathbf{C}^{-1} \mathbf{b}$; substituting the solution into Eq. (A10), we obtain the closed form of the **projector**, shown as follows:

$$\text{proj}_{M(\mathbf{C})}(\mathbf{b}, \text{col}(\mathbf{G})) = \mathbf{G} (\mathbf{G}^H \mathbf{C}^{-1} \mathbf{G})^{-1} \mathbf{G}^H \mathbf{C}^{-1} \mathbf{b}. \tag{A14}$$

The given projector is a powerful tool for solving non-white Gaussian problems, and we name it Mahalanobis projector hereafter. The properties of Mahalanobis projector are listed as follows.

Theorem I: Similar to its counterpart in Euclidean space, Mahalanobis projector is idempotent and self-adjoint in the sense of weighted inner product, shown as follows:

$$\left(\text{proj}_{M(\mathbf{C})}(\cdot, \text{col}(\mathbf{G})) \right)^2(\mathbf{x}) = \text{proj}_{M(\mathbf{C})}(\mathbf{x}, \text{col}(\mathbf{G})). \tag{A15}$$

$$\left\langle \text{proj}_{M(\mathbf{C})}(\mathbf{x}, \text{col}(\mathbf{G})), \mathbf{y} \right\rangle_{\mathbf{C}^{-1}} = \left\langle \mathbf{x}, \text{proj}_{M(\mathbf{C})}(\mathbf{y}, \text{col}(\mathbf{G})) \right\rangle_{\mathbf{C}^{-1}}, \tag{A16}$$

Theorem II: The Pythagorean Theorem on Mahalanobis distance. Mahalanobis projector can decompose a vector in the sense of weighted inner product, shown as follows:

$$\left\| \text{proj}_{M(\mathbf{C})}(\mathbf{y}, \text{col}(\mathbf{G})) \right\|_{\mathbf{C}^{-1}}^2 + \text{dist}_{M(\mathbf{C})}^2(\mathbf{y}, \text{proj}_{M(\mathbf{C})}(\mathbf{y}, \text{col}(\mathbf{G}))) = \|\mathbf{y}\|_{\mathbf{C}^{-1}}^2. \quad (\text{A17})$$

Theorem III: The Mahalanobis projector can be equivalently written as the combination of a pre-whitening filter and the projector in Euclidean space, shown as follows:

$$\text{proj}_{M(\mathbf{C})}(\mathbf{b}, \text{col}(\mathbf{G})) = \mathbf{C}^{1/2} \text{proj}_E(\mathbf{C}^{-1/2} \mathbf{b}, \text{col}(\mathbf{C}^{-1/2} \mathbf{G})). \quad (\text{A18})$$

Theorem IV: Given that the projectors are idempotent, according to [28], the projector on Euclidean space satisfies the following condition that the random vector follows $\mathbf{b} \in \mathcal{CN}(\mathbf{0}, \mathbf{I})$:

$$\|\text{proj}_E(\mathbf{b}, \text{col}(\mathbf{G}))\|^2 \sim \chi^2(2\text{rank}(\mathbf{G})). \quad (\text{A19})$$

where $\chi^2(p)$ denotes the chi-square distribution with p degrees of freedom. Based on Theorem III, we have an analogue of Eq. (A19) shown as follows:

$$\left\| \text{proj}_{M(\mathbf{C})}(\mathbf{d}, \text{col}(\mathbf{G})) \right\|_{\mathbf{C}^{-1}}^2 \sim \chi^2(2\text{rank}(\mathbf{G})), \quad (\text{A20})$$

where \mathbf{d} is a random vector follows $\mathcal{CN}(\mathbf{0}, \mathbf{C})$.

The theorems listed above can be proved with ease by substituting Eqs. (A5)–(A14) into Eqs. (A16)–(A20).

REFERENCES

1. Fishler, E., A. M. Haimovich, and R. S. Blum, "MIMO radar: An idea whose time has come," *Proceeding of 2004 IEEE Radar Conference*, 71–78, 2004.
2. Haimovich, A. M., R. S. Blum, and L. Cimini, "MIMO radar with widely separated antennas," *IEEE Signal Processing Magazine*, Vol. 25, No. 1, 116–129, 2008.
3. Fishler, E., A. M. Haimovich, and R. S. Blum, "Spatial diversity in radars-models and detection performance," *IEEE Transaction on Signal Processing*, Vol. 54, No. 3, 823–838, 2006.
4. Janatian, N., M. Modarres-Hashemi, and A. Sheikhi, "CFAR detectors for MIMO radars," *Circuits, Systems, and Signal Processing*, Vol. 32, No. 3, 1389–1418, 2013.
5. Sammartino, P. F., C. J. Baker, and H. D. Griffiths, "Target model effects on MIMO radar performance," *Proceedings of 2006 IEEE International Conference on Acoustics, Speech and Signal Processing*, V1129–V1132, 2006.
6. Petillot, Y., C. Du, and J. S. Thompson, "Predicted detection performance of MIMO radar," *Signal Processing Letters, IEEE*, Vol. 15, 83–86, 2008.
7. Blum, R. S., "Limiting case of a lack of rich scattering environment for MIMO radar diversity," *Signal Processing Letters, IEEE*, Vol. 16, No. 10, 901–904, 2009.
8. Tarokh, V., N. Seshadri, and A. R. Calderbank, "Space-time codes for high data rate wireless communication: Performance criterion and code construction," *IEEE Transactions on Information Theory*, Vol. 44, No. 2, 744–765, 1998.
9. Tarokh, V., H. Jafarkhani, and A. R. Calderbank, "Space-time block codes from orthogonal designs," *IEEE Transactions on Information Theory*, Vol. 45, No. 5, 1456–1467, 1999.
10. Tang, J., L. Ning, W. Yong, et al., "On detection performance of MIMO radar: A relative entropy-based study," *IEEE Signal Processing Letters*, Vol. 16, No. 3, 184–187, 2009.
11. Sheikhi, A., A. Zamani, and Y. Norouzi, "Model-based adaptive target detection in clutter using MIMO radar," *2006 CIE'06. International Conference on Radar*, 1–4, 2006.
12. Conte, E., A. De Maio, and C. Galdi, "Statistical analysis of real clutter at different range resolutions," *IEEE Transactions on Aerospace and Electronic Systems*, Vol. 40, No. 3, 903–918, 2004.
13. Farina, A., F. Gini, M. V. Greco, et al., "High resolution sea clutter data: statistical analysis of recorded live data," *IEE Proceedings, Radar, Sonar Navigation*, Vol. 144, No. 3, 121–130, 1997.

14. Sammartino, P. F., C. J. Baker, and H. D. Griffiths, "MIMO radar performance in clutter environment," *2006 CIE'06. International Conference on Radar*, 1–4, 2006.
15. Sammartino, P. F., C. J. Baker, and H. D. Griffiths, "Adaptive MIMO radar system in clutter," *2007 IEEE Conference on Radar*, 276–281, 2007.
16. Akcakaya, M., M. Hurtado, and A. Nehorai, "MIMO radar detection of targets in compound-Gaussian clutter," *2008 IEEE 42nd Asilomar Conference on Signals, Systems and Computers*, 208–212, 2008.
17. Chong, C. Y., F. Pascal, J. P. Ovarlez, et al., "MIMO radar detection in non-Gaussian and heterogeneous clutter," *IEEE Journal of Selected Topics in Signal Processing*, Vol. 4, No. 1, 115–126, 2010.
18. Cui, G., L. Kong, and X. Yang, "GLRT-based detection algorithm for polarimetric MIMO radar against SIRV clutter," *Circuits, Systems, and Signal Processing*, Vol. 31, No. 3, 1033–1048, 2012.
19. Gogineni, S. and A. Nehorai, "Polarimetric MIMO radar with distributed antennas for target detection," *IEEE Transaction on Signal Processing*, Vol. 58, No. 3, 1689–1697, 2010.
20. Xiao, J. and A. Nehorai, "Polarization optimization for scattering estimation in heavy clutter," *2008 IEEE International Conference on Acoustics, Speech and Signal Processing*, 1473–1476, 2008.
21. Zhang, X., D. Cao, and L. Xu, "Joint polarisation and frequency diversity for deceptive jamming suppression in MIMO radar," *Radar, Sonar & Navigation, IET*, Vol. 13, No. 2, 263–271, 2019.
22. Pirrone, D., F. Bovolo, and L. Bruzzone, "A novel framework based on polarimetric change vectors for unsupervised multiclass change detection in dual-pol intensity SAR images," *IEEE Transactions on Geoscience and Remote Sensing*, 1–16, 2020.
23. Gogineni, S. and A. Nehorai, "Game theoretic design for polarimetric MIMO radar target detection," *Signal Processing*, Vol. 92, No. 5, 1281–1289, 2012.
24. Jian, L. and P. Stoica, *MIMO Radar Signal Processing*, John Wiley & Sons, Inc., New Jersey, 2008.
25. Guoling, C., K. Lingjiang, Y. Xiaobo, et al., "The Rao and Wald tests designed for distributed targets with polarization MIMO radar in Compound-Gaussian clutter," *Circuits, Systems, and Signal Processing*, Vol. 31, No. 1, 237–254, 2012.
26. Miyamoto, T., S. Noguchi, and H. Yamashita, "Selection of an optimal solution for multi-objective electromagnetic apparatus design based on game theory," *IEEE Transactions on Magnetics*, Vol. 44, No. 6, 1026–1029, 2008.
27. Ferreira Touma, D. W. et al., "Optimizing transcutaneous energy transmitter using game theory," *IEEE Transactions on Magnetics*, 2015.
28. Wang, J., A. Dogandzic, and A. Nehorai, "Maximum likelihood estimation of compound-Gaussian clutter and target parameters," *IEEE Transactions on Signal Processing*, Vol. 54, No. 10, 3884–3898, 2006.
29. Shang, X. Q. and H. J. Song, "Radar detection based on compound-Gaussian model with inverse gamma texture," *IET Radar Sonar Navig.*, Vol. 5, No. 3, 315–321, 2011.
30. Shang, X. Q., H. J. Song, Y. Wang, and C. P. Hao, "Adaptive detection of distributed targets in compound-Gaussian clutter with inverse gamma texture," *Digit. Signal Process*, Vol. 22, No. 6, 1024–1030, 2012.
31. Park, H. R., J. Li, and H. Wang, "Polarization-space-time domain generalized likelihood ratio detection of radar targets," *Signal Process.*, Vol. 41, No. 2, 153–164, 1995.
32. Zhao, Y. N., F. C. Li, and X. L. Qiao, "Knowledge-based adaptive polarimetric detection in heterogeneous clutter," *J. Syst. Eng. Electron.*, Vol. 25, No. 3, 434–442, 2014.
33. Bon, N., A. Khenchaf, and R. Garello, "GLRT subspace detection for range and Doppler distributed targets," *IEEE Trans. Aerosp. Electron. Syst.*, Vol. 4, No. 22, 678–696, 2008.